

Sulfur, Chlorine, and Argon Abundances in Planetary Nebulae. III: Observations and Results for a Final Sample

K.B. Kwitter¹

Department of Astronomy, Williams College, Williamstown, MA 01267;
kkwitter@williams.edu

R.B.C. Henry^{1,2}

Department of Physics & Astronomy, University of Oklahoma, Norman, OK 73019;
henry@mail.nhn.ou.edu

and

J.B. Milingo^{1,2}

Department of Physics, Gettysburg College, Gettysburg, PA 17325;
jmilingo@gettysburg.edu

Received _____; accepted _____

To appear in *PASP*

ABSTRACT

This paper is the fourth in a series whose purpose is to study the interstellar abundances of sulfur, chlorine, and argon in the Galaxy using a sample of 86 planetary nebulae. Here we present new high-quality spectrophotometric observations of 20 Galactic planetary nebulae with spectral coverage from 3700–9600 Å. A major feature of our observations throughout the entire study has been the inclusion of the near-infrared lines of [S III] $\lambda\lambda 9069, 9532$, which allows us to calculate accurate S⁺² abundances and to either improve upon or convincingly confirm results of earlier sulfur abundance studies. For each of the 20 objects here we calculate ratios of S/O, Cl/O, and Ar/O and find average values of S/O=1.1E-2±1.1E-2, Cl/O=4.2E-4±5.3E-4, and Ar/O=5.7E-3±4.3E-3. For six objects we are able to compare abundances of S⁺³ calculated directly from available [S IV] 10.5 μ measurements with those inferred indirectly from the values of the ionization correction factors for sulfur. In the final paper of the series, we will compile results from all 86 objects, search for and evaluate trends, and use chemical evolution models to interpret our results.

Subject headings: ISM: abundances – planetary nebulae: general – planetary nebulae: individual – stars: evolution

¹Visiting Astronomer, Kitt Peak National Observatory, National Optical Astronomy Observatories, which is operated by the Association of Universities for Research in Astronomy, Inc. (AURA) under cooperative agreement with the National Science Foundation

²Visiting Astronomer, Cerro Tololo Interamerican Observatory, National Optical Astronomy Observatories, which is operated by the Association of Universities for Research in

1. INTRODUCTION

This is the fourth paper in a project to study abundances in planetary nebulae (PNe), highlighting the elements sulfur, chlorine, and argon. The motivation to focus on these three elements has been the realization that their abundances are unaffected by nucleosynthesis in the progenitors of PNe. In contrast to elements like carbon, nitrogen, and oxygen, whose current nebular abundances can be profoundly different from those in the original star, the sulfur, chlorine and argon abundances we measure now in a nebula are representative of the original composition of the progenitor star. In this way, PNe can provide information on both current and past chemical composition of the interstellar medium in the Galaxy, and can be used to evaluate theoretical yield predictions from stellar evolution models.

The three preceding papers in this series (Kwitter & Henry 2001 [Paper I], Milingo et al. 2001 [Paper IIA], and Milingo, Henry, & Kwitter 2001 [Paper IIB]) have reported spectrophotometry and abundance analyses of a total of 56 primarily type II (disk) PNe in our Galaxy. In the present paper we present new spectrophotometry and abundances for 20 more objects. In the final paper, we will also include results from 10 PNe originally observed for another project, bringing the total in our sample to 86.

In §2 we describe the observations and data, and in §3 we present our results; a summary is given in §4.

Astronomy, Inc. (AURA) under cooperative agreement with the National Science Foundation.

2. DATA

Table 1 lists the objects discussed in this paper. Column 1 gives the object name, column 2 the angular size, column 3 the slit offset, if any, and columns 4 and 5 the blue and red exposure times, respectively. Column 6 contains either K or C denoting optical/near-infrared spectrophotometry obtained at Kitt Peak or Cerro Tololo, respectively. Six PNe have available ISO SWS observations that include the [S IV] 10.5μ line, which we discuss in §2.2; these objects are listed first in Table 1 and the ISO exposure times are given in the last column.

2.1. Optical and Near-Infrared Observations

Observations at CTIO were obtained in March 1997 using the 1.5m telescope and cassegrain spectrograph with Loral 1K CCD. The 1200 x 800 Loral 1K CCD has 15μ pixels. We used a $5'' \times 320''$ extended slit in the E-W direction. Perpendicular to dispersion the scale was $1.3''/\text{pixel}$. Gratings #22 and #9 were used to obtain extended spectral coverage from 3600-9600 Å with overlap in the H α region. Both gratings have nominal wavelength dispersions of 2.8 Å/pixel and 8.6 Å FWHM resolution.

Data for objects observed at KPNO were obtained in May 1996, December 1996, or June 1999 with the Goldcam CCD spectrometer at the 2.1m telescope. The chip was a Ford 3K \times 1K CCD with 15μ pixels. We used a slit that was 5'' wide and extended 285'' in the E-W direction, with a spatial scale of $0''.78/\text{pixel}$. The 3700-9600Å range, overlapping coverage from $\sim 5750 - 6750\text{\AA}$, was covered with two gratings. For the blue, we used #240 and a WG345 order-separation filter; wavelength dispersion was 1.5 Å/pixel (~ 8 Å FWHM resolution). For the red we used grating #58 with an OG530 order-separation filter, yielding 1.9 Å/pixel (~ 10 Å FWHM resolution).

Both CTIO and KPNO CCD's produced fringing at wavelengths beyond \sim 7500 Å. Assuming less than ideal fringe removal via dome flats, the fringe amplitudes range from roughly $\pm 1\%$ at 7500 Å, to $\pm 9.8\%$ at 9500 Å, the longest wavelength we measure. We note this contribution to the uncertainty in our line intensities measured at wavelengths longer than 7500 Å.

Many of these PNe are relatively small in angular size; in those cases, we placed the spectrograph slit on the brightest part of the nebula as seen on the acquisition screen, avoiding the central star if it was visible. We obtained the usual bias and twilight flat-field frames each night, along with HeNeAr comparison spectra for wavelength calibration and standard star spectra for sensitivity calibration. The original two-dimensional spectra were reduced and calibrated using standard long-slit spectrum reduction methods in IRAF³. One-dimensional spectra were extracted from the original two-dimensional images interactively using the *kpnoslit* package. Line fluxes were measured with *splot*.

Our measured line strengths are tabulated in Tables 2A-C. For each line identification in the first column we list the relative extinction factor $f(\lambda)$ followed by two columns for each object containing the observed $[F(\lambda)]$ and dereddened $[I(\lambda)]$ line strengths normalized to $H\beta=100$. Observed fluxes were dereddened using the extinction curve of Savage & Mathis (1979), where each dereddened intensity was obtained by multiplying the observed flux by the factor 10^{cf_λ} , where c is the logarithmic extinction factor and f_λ is the reddening coefficient. We assumed $H\alpha/H\beta=2.86$ (Hummer & Storey 1987). Values for the logarithmic extinction factor c and $\log F_{H\beta}$ in erg cm⁻² s⁻¹, the $H\beta$ flux as measured through the slit are found at or near the bottom of each table. Estimated uncertainties for line strengths

³IRAF is distributed by the National Optical Astronomy Observatories, which is operated by the Association of Universities for Research in Astronomy, Inc. (AURA) under cooperative agreement with the National Science Foundation.

are represented using colons, as defined in the table footnotes.

To test the accuracy of our extinction factor, c , we determined separate values using the Paschen 10 and Paschen 8 lines at 9014\AA and 9546\AA , respectively. Ideally, these c values should match the one inferred using $\text{H}\alpha$, i.e. the one listed in the line strength tables. This comparison is shown in Table 3A, where for each object we list the three values of c . Recombination data required for this exercise were taken from Osterbrock (1989, Table 4.4). These values are further compared in Fig. 1, where we plot $c(\text{P}10)$ or $c(\text{P}8)$ versus $c(\text{H}\alpha)$ and include a straight line to show the ideal one-to-one relation. Overall, the trend is as anticipated, but with a typical difference of ~ 0.15 between $c(\text{H}\alpha)$ and either $c(\text{P}10)$ or $c(\text{P}8)$.

As a check on the quality of the data and measuring accuracy, we list in Table 3B our measurements for several line ratios predicted by theory to have constant values. These ratios are identified in the table footnote. The last two lines of the table give our observed mean and the theoretical (expected) value. With the exception of the [Ne III] ratio, agreement is good.

In §3 we employ the dereddened intensities to determine electron temperatures, densities, and abundances.

2.2. ISO Data

We were able to obtain pre-publication estimates of ISO SWS fluxes for [S IV] 10.5μ and $\text{Br}\alpha 4.05\mu$ for the six PNe in Table 2A (Barlow & Liu, private communication; Beintema & Salas, private communication). These observed fluxes are listed near the bottom of Table 2A. We joined them to the optical spectrum in the following way. To correct the observed ratio $I(10.5\mu)/\text{Br}\alpha$ for differential interstellar extinction, we used the

infrared extinction law, $A(\lambda)/A(V)$ given by Rieke & Lebofsky (1985): for $\text{Br}\alpha$ and 10.5μ the values are 0.04 and 0.08, respectively. Combined with our value for c determined from the Balmer lines, we took $c = 1.41E(B-V)$, and \mathbf{R} , the ratio of total to selective extinction = 3.1, to calculate $A(V)$. The resulting values for $A(\text{Br}\alpha)$ and $A(10.5\mu)$ are shown near the bottom of Table 2A. For an electron temperature of 10,000 K, and a density of 1000 cm^{-3} , the predicted ratio of $\text{Br}\alpha/\text{H}\gamma = 0.17$, and $\text{H}\gamma/\text{H}\beta = 0.46$ (Hummer & Storey 1987). We multiplied the reddening-corrected $[\text{S IV}]/\text{Br}\alpha$ ratios by $0.17 \times 0.46 = 0.078$ to yield $I(\lambda)$ values for $[\text{S IV}]$, which are given (relative to $\text{H}\beta=100$) in Table 2A.

The fluxes for $[\text{Ar III}] 8.99\mu$ were also available for this set of six PNe (Barlow & Liu, private communication; Beintema & Salas, private communication). These were corrected for extinction $[A(\lambda)/A(V)]$ for $8.99\mu = 0.07$; Reike & Lebofsky 1985] and converted to a ratio with $\text{H}\beta$ in a manner analogous with the $[\text{S IV}] 10.5\mu$ line described above. These data are also presented near the bottom of Table 2A.

3. RESULTS

Electron temperatures, densities, as well as ion and elemental abundances were calculated using exact routines employed in Papers I and IIB. The reader is referred to Paper I, where our methods are described in detail. To summarize the methods, temperatures and densities were computed in the standard fashion, using forbidden line ratios which are sensitive to the respective quantity. For ion abundances, we employed a program which utilizes a 5-level atom equilibrium calculation to compute abundances from forbidden lines of heavy elements. Ions of H and He were determined from permitted line strengths using effective recombination coefficients. The sum of abundances of observed ions for an element was then corrected for unseen ions through the use of ionization correction factors (ICF) described in detail in Paper I to obtain total elemental abundances.

Temperatures, densities, ion abundances, and ICFs are listed by object in Tables 4A-C. Uncertainties are described in the table footnotes. Temperatures which appear to be anomalously high are enclosed in parentheses. For K648 and NGC 2242, we were unable to determine a [S II] electron density directly from our data, because strengths for one or both of the 6716 Å and 6732 Å lines was undetected. In this case, densities reported in earlier papers were adopted, as indicated in footnotes to the relevant tables. A major feature of our work in this series of papers is to use the near-infrared (NIR) forbidden lines of [S III] at $\lambda\lambda 9069, 9532$ along with $\lambda 6312$ to derive S⁺² abundances using a [S III] temperature where possible. In a few cases where this temperature differed by more than 5,000 K from the [O III] temperature, we adopted the [N II] temperature as more representative of the S⁺² zone. For NGC 1535 (Table 4C), however, the [N II] value appeared to be suspiciously high, so in this case we used the [O III] temperature.

As a check on our S⁺² measurements, we also calculated the abundance of this ion using the [S III] $\lambda 6312$ line and (usually) the [N II] temperature. These results are included in Table 4A-C. Although the $\lambda 6312$ line is much weaker than the nebular [S III] lines in the NIR, it is generally more accessible spectroscopically, and thus has been used extensively to calculate S⁺² abundances (cf. Kingsburgh & Barlow 1994). We plot the two abundances against each other in Fig. 2 and include a straight line to show the ideal one-to-one correspondence. As we have also found in Papers I and IIB, the NIR lines tend to yield lower abundances for this ion. This could result from the fact that when [S III] $\lambda 6312$ is used, the [S III] temperature is generally unavailable, and one is forced to employ either the [O III] or [N II] temperature. Since generally we found these temperatures to be somewhat lower than the [S III] temperature in the cases where all three could be determined, that would explain the higher S⁺² abundances when the [S III] temperature was unavailable.

As a first-order check on our sulfur ICF, we were able to use the ISO data described

above for the six PNe in Table 4A to calculate the ionic abundance of S^{+3} from the [S IV] 10.5μ line, using collision strengths and transition rates from Mendoza (1983). These results, labelled “IR” are compared in Table 5 with S^{+3} abundances inferred by assuming that $S^{+3} = (S^{+2} + S^+) \times (ICF - 1)$, labelled “ICF.” The fourth column in the table lists the ratio of ICF/IR abundances. If the methods agreed perfectly, then values in this column would be unity; clearly this is not the case. Some of the variance is surely due to the uncertainties in the values in Table 5, but this is likely not the whole explanation. It is always risky to compare observations of an extended PN obtained through apertures that differ in size and/or placement. We note that there are significant differences in the nebular area sampled by the two kinds of observations presented here: the ISO SWS aperture is roughly $20'' \times 33''$ (with some dependence on wavelength), while our observations were made through a $5''$ -wide slit. Except for Hb 12, which is notoriously inhomogeneous (Hyung & Aller 1996), and where the (uncertain) ICF value of S^{+3}/H^+ is about eight times that indicated by the (very uncertain) 10.5μ line, the ratios for the other PNe, some also fairly uncertain, range from 0.22 to 0.88. So, while not as close as one might wish, the values in Table 5 are not excessively discordant, considering the uncertainties in the ISO calibrations, in the conversion of infrared fluxes to intensity ratios with $H\beta$, and in the different nebular areas sampled.

As a second comparison with ISO data, we used fluxes for the [Ar III] 8.99μ line. In Table 4A we list the Ar^{+2}/H^+ abundances calculated from the 8.99μ and 7135 \AA lines; it can be seen that all pairs of values agree to within a factor of two, and for four of the six objects, agreement is within 20%. This agreement for abundances calculated separately from observed fluxes of two lines of the same ion, is heartening. It may be that measurements of [Ar III] are less sensitive than [S IV] to differing slit sizes and positions. In conclusion, while agreement between abundances of S^{+3} and Ar^{+2} inferred from ICF predictions and derived directly from observations is encouraging, uncertainties introduced

by the differences in aperture size make it difficult to make a more detailed assessment.

Elemental abundances for all 20 objects are listed in Tables 6A-C. The last two columns of each table give solar and Orion Nebula abundances for comparison, where these have been taken from Grevesse et al. (1996) and Esteban et al. (1998), respectively. In all cases the sulfur abundance is based upon the use of S^+ and S^{+2} , along with the relevant ICF. In Table 6A we also list the final sulfur abundance determined using the S^{+3} reported in Table 4A for comparison. Clearly, the discrepancies associated with S^{+3} that were noted when the ion abundances were considered above have been suppressed because of the dominant influence of the S^{+2} abundance.

The ratios of S/O, Cl/O and Ar/O are plotted against O/H in Fig. 3. Results from this paper are shown with filled circles, while results from Paper I are shown with open circles. In each panel the sun's position is indicated with a star, while that of Orion is shown with an 'X'. Typical uncertainties are indicated and explained in the caption. Clearly there is good agreement between samples. We also point out the anomalously high values for S/O and Ar/O for Hb12, the PN with the lowest value for O/H. It is possible that our estimate of O/H is too low, although we point out that Cl/O appears consistent with the remainder of the sample.

Finally, Table 7 lists unweighted averages and standard deviations for the sample in this paper as well as the samples in Papers I and IIB. For comparison, we also give the averages found by Kingsburgh & Barlow (1994; KB) and Aller & Keyes (1987; AK) as well as solar and Orion values. We note that all of our averages compare favorably with these other results, considering all of the uncertainties.

As we have seen previously, the ratios S/O, Cl/O, and Ar/O appear to be constant over the metallicity range as gauged by O/H. This is consistent with the idea that these four elements are formed by stars belonging to the same mass range. In our final paper in

the series we plan to explore this idea in detail, employing chemical evolution models in order to evaluate current predictions of stellar nucleosynthesis.

4. SUMMARY

In this, the fourth paper in a series investigating the abundances of S, Cl, and Ar in planetary nebulae and the Galactic interstellar medium, we report on spectrophotometric observations of 20 Galactic PNe, where our spectral coverage extended from 3700-9600 Å. We also calculate electron temperatures and densities, as well as ion and element abundances for each object. We find average values of $S/O=1.1E-2\pm1.1E-2$, $Cl/O=4.2E-4\pm5.3E-4$, and $Ar/O=5.7E-3\pm4.3E-3$ for our sample. These numbers agree very well with our results in the previous papers in the series and with determinations made by others. One of the major features of our current work is to use the NIR lines of [S III] $\lambda\lambda 9069, 9532$ along with [S III] temperatures to calculate sulfur abundances. This is the first time these lines have been used to determine sulfur abundances in such a large PN sample.

In the next (final) paper we will compile results from all papers in this series and search for trends among the data. In addition, we plan to apply chemical evolution models to our data in an attempt to evaluate the quality of published stellar yields for O, S, Cl, and Ar, as well as to assess the role of Type Ia supernovae in the cosmic buildup of these four elements.

We thank the TACs at KPNO & CTIO for granting us observing time, to the local staff there for their assistance, and to the IRAF staff for their ready answers. We are extremely grateful to M.J. Barlow and X.-W.Liu and to D. Beintema and J.B. Salas for providing the ISO SWS line fluxes. Our research is supported by NSF grant AST-9819123.

Table 1. Object Data and Observation Information

Object	Angular Diameter (''') ^a	Offset ('')	Blue Exp (sec)	Red Exp (sec)	Observatory ^b	ISO SWS Exp (sec)
Hb 12	1	...	325	75	K	1912
NGC 3918	19	...	100	720	C	1140
NGC 5882	14	...	390	480	C	1030
NGC 6567	7.6	...	390	330	C	1030
NGC 6578	8.5	...	1180	300	C	1030
NGC 7662	17 ^b	3S	90	100	K	1912
BB 1	3	...	600	1200	K	...
H4-1	2.7	...	1200	2700	K	...
Hu2-1	2.6	...	300	1680	K	...
IC 2165	9	...	330	90	K	...
J900	9	...	120	120	K	...
K648	1	...	1800	2400	K	...
NGC 40	48	14.2N	600	600	K	...
NGC 650A	67	9N	600	900	K	...
NGC 650B	67	21S,24W	600	600	K	...
NGC 1535	21	8N	510	600	K	...
NGC 2022	19	6.3S	900	900	K	...
NGC 2242	22	...	600	600	K	...
NGC 2371	44	9.7S,15.7W	300	300	K	...
NGC 2438	64	16.3N	300	300	K	...
NGC 2440	16	4S	100	360	K	...
NGC 7027	14	...	25	110	K	...

^aTaken from Acker et al. (1992)^bK=KPNO, C=CTIO^cBright inner shell only

Table 2A. Line Strengths^a

Line	f(λ)	F(λ)	I(λ)	F(λ)	I(λ)	F(λ)	I(λ)	F(λ)	I(λ)	F(λ)	I(λ)	F(λ)	I(λ)
[O II] λ3727	0.29	7.2	14.6	62.0	74.4	11.3	14.9	15.6	25.0	7.5	19.1	6.5	6.6
He II + H10 λ3797	0.27	2.6	5.0	3.8	4.5	3.2	4.2	1.9	4.5	4.0	4.0
He II + H9 λ3835	0.26	3.7	7.0	5.2	6.1	2.3:	3.5:	2.5	5.8	6.1	6.2
[Ne III] λ3869	0.25	34.0	62.6	105	123	70.7	89.6	43.5	65.3	30.4	68.0	76.0	77.5
He I + H8 λ3889	0.25	7.7	14.0	16.7	19.5	15.3	19.3	10.2	15.2	10.0	22.0	15.0	15.3
Hε + [Ne III] λ3968	0.22	22.0	37.9	48.6	55.9	36.0	44.4	17.1	24.6	18.8	38.5	39.0	39.7
He I + He II λ4026	0.21	1.7	2.8	1.8	2.1	1.9:	2.3	1.5	2.1	1.6	3.1	1.5	1.5
[S II] λ4072	0.20	1.2	1.9	2.5	2.8	0.9:	1.0:	0.9:	1.2:	0.9:	1.7:	1.4	1.4
He II + Hδ λ4101	0.19	16.0	25.2	25.7	28.9	22.7	27.1	15.3	20.7	15.3	27.9	26.0	26.4
He II λ4198	0.16	0.5::	0.6::	0.9	0.9
C II λ4267	0.14	0.1::	0.2::	0.3	0.3	0.3	0.4	0.4::	0.5::	0.9:	1.4:	0.3::	0.3::
Hγ λ4340	0.12	33.4	45.1	43.8	47.3	41.0	46.1	36.6	44.7	32.9	48.9	44.0	44.4
[O III] λ4363	0.12	11.5	15.3	19.3	20.8	4.8	5.4	7.6	9.2	1.6	2.3	16.0	16.1
He I λ4471	0.09	4.2	5.2	3.1	3.3	4.9	5.3	4.5	5.2	4.7	6.3	2.4	2.4
He II λ4540	0.07	1.6	1.7	2.1	2.1
N III λ4640	0.05	0.9::	1.0::	6.0	6.2	3.0	3.2	1.7	1.8	3.4	4.0	4.7	4.7
He II λ4686	0.04	46.0	47.0	3.6	3.7	1.4	1.5	1.4	1.6	60.0	60.2
He I + [Ar IV] λ4711	0.03	0.8	0.9	7.8	7.9	3.0	3.1	1.4	1.5	1.4	1.5	7.3	7.3
[Ne IV] λ4724	0.03	0.4	0.4
[Ar IV] λ4740	0.02	0.2::	0.2::	6.9	7.0	3.0	3.0	1.0	1.0	1.0	1.1	6.5	6.5
Hβ λ4861	0.00	100	100	100	100	100	100	100	100	100	100	100	100
He I λ4922	-0.02	1.4	1.3	0.3::	0.3::	1.0::	1.0::	1.0::	1.0::	1.5:	1.4:	0.4	0.4
[O III] λ4959	-0.03	160	149	538	528	354	344	326	311	299	272	372	371
[O III] λ5007	-0.04	515	466	1625	1583	1087	1045	1016	950	944	827	1112	1116
[N I] λ5199	-0.09	0.5::	0.4::	0.7::	0.7::	0.1::	0.1::
He II λ5411	-0.13	4.2	3.9	0.3	0.3	0.1::	4.9	4.9
[Cl III] λ5517	-0.16	0.1::	0.1::	0.7	0.6	0.4	0.4	0.4:	0.3:	0.6	0.4	0.5	0.5
[Cl III] λ5537	-0.16	0.2::	0.1::	1.0	0.9	0.6	0.5	0.4:	0.3:	0.8	0.5	0.5	0.5
[N II] λ5755	-0.21	12.3	7.5	2.0	1.8	0.3	0.2	0.8:	0.6:	0.6	0.3
C IV λ5806	-0.22	0.3	0.3	0.5	0.4	5.0	3.5	2.3	1.1

Table 2A—Continued

Table 2A—Continued

	Hb12		NGC 3918		NGC 5882		NGC 6567		NGC 6578		NGC 7662		
Line	f(λ)	F(λ)	I(λ)										
[Ar III] $\lambda 7751$	-0.54	18.0	4.9	6.0	4.3	5.8	3.5	2.8	1.2	17.7	3.2	2.2	2.2
[Cl IV] $\lambda 8045$	-0.57	0.5	0.1	1.5	1.1	1.2	0.7	0.7:	0.3:	1.6:	0.3:	1.4	1.3
He II $\lambda 8236$	-0.59	1.6	1.1	0.2:	0.1	1.4	1.3
P17 $\lambda 8467$	-0.62	2.2:	0.5:	0.5:	0.3:	0.6:	0.4:	2.1:	0.3:	0.3:	0.3:
P16 $\lambda 8502$	-0.62	3.3:	0.7:	0.6:	0.4:	0.8:	0.4:	1.1:	0.4:	2.9:	0.4:	0.5:	0.5:
P15 $\lambda 8544$	-0.63	3.8:	0.8:	0.8:	0.5:	1.0:	0.6:	1.3:	0.5:	3.3:	0.4:	0.5:	0.5:
P14 $\lambda 8598$	-0.63	4.3:	0.9:	0.9:	0.6:	1.1:	0.6:	1.3:	0.5:	4.0:	0.5:	0.8:	0.8:
P13 $\lambda 8664$	-0.64	5.3:	1.1:	1.2:	0.8:	1.5:	0.8:	3.1:	1.1:	5.3:	0.7:	1.1:	1.0:
P12 $\lambda 8750$	-0.64	6.1:	1.3:	1.4:	0.9:	1.8:	1.0:	3.5:	1.2:	5.8:	0.7:	1.2:	1.1:
P11 $\lambda 8862$	-0.65	7.8:	1.6:	2.2:	1.5:	2.6:	1.4:	3.1:	1.1:	8.0:	1.0:	1.8:	1.7:
P10 $\lambda 9014$	-0.67	10.0	2.0	2.5	1.6	3.1	1.6	4.0	1.4	10.4	1.2	2.5	2.4
[S III] $\lambda 9069$	-0.67	117	23.1	25.2	16.6	29.0	15.5	20.6	7.0	158	18.6	14.0	13.3
P9 $\lambda 9228$	-0.68	15.0:	2.9:	4.7:	3.1	5.4	2.9:	7.6:	2.5:	18.9:	2.2:	3.0:	2.8:
[S III] $\lambda 9532$	-0.70	258	47.5	76.7	49.6	104	54.0	64.8	21.0	455	48.8	27.0	25.6
P8 $\lambda 9546$	-0.70	19.0:	3.5:	2.1::	1.4::	3.4:	1.8:	10.4:	3.4:	9.3::	1.0::	2.5:	2.4:
[Ar III] $8.99\mu^b$			3.8:		14.1::		16.1		8.4		27.2		6.4
[S IV] $10.5\mu^b$			2.1::		122::		181		88		228::		133
c			1.05		0.27		0.41		0.70		1.39		0.03
log F _{Hβ} ^c		-10.97		-10.39		-10.65		-11.06		-11.81		-10.51	
log F _{Bra} ^d		-10.96±.04		-11.29±.09		-11.10±.01		-12.09±.04		-12.46±.09		-11.19±.03	
A(Bra) ^b		0.09		0.02		0.04		0.06		0.10		0.00	
log F _{8.99μ} ^d		-11.30±.07		-11.05::		-10.80±.01		-12.08±.05		-11.94±.04		-11.28±.04	
A(8.99 μ) ^b		0.17		0.03		0.04		0.07		0.11		0.00	
log F _{10.5μ} ^d		-11.57±.13		-10.11±.08		-9.75±.01		-11.07±.01		-11.04±.01		-9.96±.01	
A(10.5 μ) ^b		0.21		0.05		0.08		0.14		0.22		0.00	

^aA single colon indicates uncertainty between 25% and 50%; a double colon indicates uncertainty greater than 50%.

^bcalculated as described in the text

^cergs cm⁻² s⁻¹ in our extracted spectra

^dergs cm⁻² s⁻¹ through ISO aperture, provided by M. Barlow & X.-W. Liu, except for NGC 3918, supplied by D. Beintema & J.B. Salas

Table 2B. Line Strengths^a

	BB1	H4-1	Hu2-1	IC2165	J900	K648	NGC 650A	NGC 650B									
Line	f(λ)	F(λ)	I(λ)	F(λ)	I(λ)	F(λ)	I(λ)	F(λ)	I(λ)	F(λ)	I(λ)	F(λ)	I(λ)	F(λ)	I(λ)		
[O II] λ3727	0.29	12.9	12.9	183	193	58.2	77.2	30.2	39.6	40.2	55.7	32.0	35.9	237	250	453.0	521.3
He II + H10 λ3797	0.27	3.6	3.6	4.2	4.4	3.5	4.5	3.6	4.6	3.4	4.6	3.0::	3.2::	3.3	3.8
He II + H9 λ3835	0.26	8.9	8.9	6.5	6.8	5.1	6.6	7.6	9.6	6.9:	9.2:	1.8	2.0	8.0	8.4	7.6	8.6
[Ne III] λ3869	0.25	201	201	5.0	5.2	13.9	17.7	78.8	99.7	69.1	91.5	11.6	12.8	126	132	144	163
He I + H8 λ3889	0.25	20.7	20.7	22.5	23.5	11.6	14.7	14.1	17.8	12.7	16.7	16.6	18.3	17.4	18.3	18.0	20.3
He ϵ + [Ne III] λ3968	0.22	119	119	17.1	17.8	17.6	21.9	60.4	74.5	52.3	67.2	4.6	5.0	85.9	89.6	94.4	105
He I + He II λ4026	0.21	2.0	2.0	2.6::	2.7::	1.6	2.0	1.3	1.6	1.1:	1.4:	1.1::	1.2::	1.6	1.7
[S II] λ4072	0.20	1.4:	1.4:	0.6::	0.6::	1.2	1.4	1.7	2.1	1.6:	2.0:	4.4	4.6	7.1	7.8
He II + Hδ λ4101	0.19	23.6	23.6	24.7	25.5	20.9	25.1	20.0	23.8	18.1	22.3	21.0	22.6	21.0	21.8	20.6	22.5
He II λ4198	0.16	0.3::	0.4::	0.7	0.8	0.7::	0.9::	0.9::	1.0::	0.3::	0.3::
C II λ4267	0.14	0.6::	0.6::	1.1	1.1	0.4:	0.4:	0.3	0.4	0.8::	0.9::	0.9	0.9	0.6	0.6	0.6::	0.6::
H γ λ4340	0.12	45.1	45.1	46.8	47.9	41.9	47.3	40.0	44.9	38.2	43.9	44.4	46.6	43.4	44.4	42.9	45.5
[O III] λ4363	0.12	4.2	4.2	8.7	8.9	2.1	2.3	14.9	16.6	9.5	10.9	2.8	2.9	10.0	10.2	8.8	9.4
He I λ4471	0.09	3.7	3.7	5.2	5.3	4.5	4.9	2.7	2.9	2.6	2.9	4.7	4.8	2.2	2.2	3.3	3.5
He II λ4540	0.07	0.8::	0.8::	1.2	1.3	1.1:	1.2:	1.6	1.6	0.9:	1.0:
N III λ4640	0.05	0.7::	0.7::	0.9	0.9	3.8	4.0	2.8	2.9
He II λ4686	0.04	20.4	20.4	9.4	9.4	0.2::	0.2::	38.5	39.8	33.8	35.2	54.6	55.0	27.9	28.4
He I + [Ar IV] λ4711	0.03	0.6::	0.6::	0.6::	0.6::	0.7	0.8	4.6	4.7	2.2	2.3	0.8	0.8	3.4	3.4	1.2	1.2
[Ne IV] λ4724	0.03	0.5	0.5	0.1::	0.1::
[Ar IV] λ4740	0.02	4.3	4.4	2.0	2.1	2.0	2.0	0.3	0.3
H β λ4861	0.00	100	100	100	100	100	100	100	100	100	100	100	100	100	100	100	100
He I λ4922	-0.02	0.7	0.7	1.2	1.2	1.2	1.1	0.8	0.8	0.7:	0.7:	0.5::	0.5::	0.5	0.5	1.0	1.0
[O III] λ4959	-0.03	89.9:	89.9:	218	217	147	143	337	328	298	288	80.7	79.8	339	337	293	289
[O III] λ5007	-0.04	304	304	663	658	456	438	1128	1085	993	948	243	239	1123	1114	961	942
[N I] λ5199	-0.09	0.3:	0.3:	0.1::	0.1::	0.4	0.4	0.4	0.4	3.2	3.1	10.0	9.6
He II λ5411	-0.13	1.7	1.7	0.6	0.6	3.8	3.4	3.4	2.9	4.9	4.8	2.2	2.1
[Cl III] λ5517	-0.16	0.1::	0.1::	0.4	0.3::	0.3::	0.2	0.9	0.8	1.0	0.9
[Cl III] λ5537	-0.16	0.3:	0.3:
[O I] λ5577	-0.17	0.1:	0.1:	0.1::	0.1::	0.5	0.5
[N II] λ5755	-0.21	0.8	0.8	2.4:	2.3:	2.8	2.3	1.4	1.2	1.3	1.0	5.5	5.3	11.2	10.1

Table 2B—Continued

	BB1	H4-1	Hu2-1	IC2165	J900	K648	NGC 650A	NGC 650B							
Line	f(λ)	F(λ)	I(λ)												
C IV λ 5806	-0.22	0.3	0.2
He I λ 5876	-0.23	11.4	11.4	15.7	15.1	18.7	15.0	10.8	8.7	11.9	9.2	14.2	13.0	7.5	7.2
He II λ 6005	-0.26	0.1:	0.1:	0.1:	0.1:	0.1:	0.1:
He II λ 6038	-0.26	0.2:	0.2:	0.1:	0.1:	0.1:	0.1:	0.1:	0.1:
He II λ 6074	-0.27	0.1:	0.1:	0.1:	0.1:	0.1:	0.1:
[Ca V] λ 6087	-0.27	0.1:	0.1:
[K IV] λ 6101	-0.28	0.3	0.3	0.1:	0.1:	0.1:	0.1:	0.2:	0.2:
He II λ 6119	-0.28	0.1	0.1	0.1:	0.1:	0.1:	0.1:
He II λ 6172	-0.29	0.2::	0.2::	0.1:	0.1:	0.1:	0.1:	0.1:	0.1:
He II λ 6235	-0.30	0.2	0.1	0.2:	0.1:	0.1:	0.1:	0.3	0.3
[O I] λ 6300	-0.31	0.8	0.8	11.7	11.1	3.1	2.3	4.1	3.0	8.6	6.1	14.6	13.8
[S III] λ 6312	-0.32	0.2::	0.2::	0.8	0.6	2.6	1.9	1.8	1.3	3.9:	3.6:
[O I] λ 6363	-0.32	0.3	0.3	3.9	3.7	0.9	0.7	1.1	0.8	2.6	1.8	4.4:	4.1:
He II λ 6407	-0.33	0.2	0.2	0.3:	0.2:	0.1:	0.1:	0.3::	0.3::
[Ar IV] λ 6436	-0.34	0.6	0.5	0.3	0.2	0.3::	0.3::
[N II] λ 6548	-0.36	9.9	9.9	34.6	32.5	29.9	21.0	18.3	13.1	17.5	11.8	98.1	91.7
H α λ 6563	-0.36	252	252	305	286	405	286	400	286	427	286	329	286	306	286
[N II] λ 6584	-0.36	28.1	28.1	118	111	89.9	63.2	49.8	35.5	55.5	37.0	4.3	3.8	310.0	289.5
He I λ 6678	-0.38	3.0	3.0	4.2	4.0	5.4	3.7	0.1	0.1	4.1	2.7	4.3	3.7	2.4	2.2
[S II] λ 6716	-0.39	0.1::	0.1::	1.1	1.1	0.6	0.4	2.4	1.7	3.6	2.4	37.8	35.2
[S II] λ 6731	-0.39	0.2::	0.2::	1.0	1.0	1.3	0.9	4.0	2.8	5.9	3.9	0.3	0.3	30.1	28.0
He II λ 6891	-0.42	0.2	0.1	0.6	0.4	0.5::	0.4::
[Ar V] λ 7005	-0.43	0.2	0.1	2.0	1.3	0.7	0.4	0.8	0.7
He I λ 7065	-0.44	4.5	4.5	5.1	4.7	13.0	8.5	7.5	4.9	6.8	4.2	1.8	1.6
[Ar III] λ 7135	-0.45	0.2	0.2	0.4	0.4	15.8	10.2	15.4	10.1	12.3	7.4	0.8	0.6	29.6	27.2
He II λ 7178	-0.46	0.2	0.2	1.1	0.7::	0.7::	0.4	0.7	0.7
[Ar IV] λ 7236	-0.47	0.2	0.2	0.5	0.5	0.7	0.4	0.4	0.3	0.9	0.6	0.6	0.5
[Ar IV] λ 7264	-0.47	0.3	0.2	0.1::	0.1::	0.1::	0.1::
He I λ 7281	-0.47	0.6	0.6	0.6	0.6	1.3	0.8	0.9	0.6	0.8	0.5	0.5	0.5
[O II] λ 7323	-0.48	1.2	1.2	8.9	8.1	45.8	28.8	8.9	5.7	15.0	8.8	4.1	3.4	8.4	7.7
														19.7	15.6

Table 2B—Continued

		BB1	H4-1	Hu2-1	IC2165	J900	K648	NGC 650A	NGC 650B								
Line		f(λ)	F(λ)	I(λ)													
[Cl IV] λ 7529	-0.51	0.1::	0.1::	0.6	0.4	0.4	0.2	
He II λ 7591	-0.52	0.4:	0.3:	0.6:	0.3:	1.0	0.9	0.7::	0.6::
[S I] λ 7726	-0.54	0.2:	0.1:	0.5	0.3
[Ar III] λ 7751	-0.54	4.0	2.4	3.9	2.4	3.3	1.8	0.4::	0.3::	7.3	6.6	9.1	7.0
[Cl IV] λ 8045	-0.57	1.5	0.9	0.8	0.4	0.6:	0.6:	0.2:	0.1:
He II λ 8236	-0.59	0.4	0.4	0.3::	0.3::	2.1	1.2	1.9	1.0	1.6	1.4	1.1	0.8
P17 λ 8467	-0.62	0.6	0.3	0.9:	0.4:	0.6:	0.5:
P16 λ 8502	-0.62	0.9	0.5	0.8	0.4	1.0:	0.5:	0.6:	0.4:
P15 λ 8544	-0.63	1.0	0.6	1.1	0.6	1.1:	0.6:	0.7:	0.5:
P14 λ 8598	-0.63	0.5:	0.5:	1.2	0.6	1.3	0.7	1.2:	0.6:	0.7:	0.5:
P13 λ 8664	-0.64	0.9:	0.9:	1.5	0.8	1.7	0.9	2.0:	1.0:	1.3:	1.1:	1.6:	1.1:
P12 λ 8750	-0.64	1.3:	1.3:	2.0	1.1	2.0	1.1	2.4:	1.2:	1.5::	1.1::	1.2:	1.1:	1.6:	1.2:
P11 λ 8862	-0.65	0.7:	0.7:	2.4	1.3	2.6	1.4	3.3:	1.6:	1.3::	1.0:	1.9:	1.7:	2.0:	1.5:
P10 λ 9014	-0.67	1.7:	1.7:	2.2	2.0	3.5	1.9	2.4	1.3	3.4:	1.6:	1.8::	1.4:	2.0:	1.8:	2.7:	1.9:
[S III] λ 9069	-0.67	0.5:	0.5:	1.0::	0.9::	9.9	5.2	35.0	18.8	25.0	11.9	44.7	39.4	52.7	38.2
P9 λ 9228	-0.68	2.9:	2.9:	3.5	3.1	5.5	2.9	7.5	4.0	7.2:	3.4:	3.4::	2.6::	4.9:	4.3:	4.7:	3.4:
[S III] λ 9532	-0.70	0.4:	0.4:	2.9	2.6	42.1	21.5	89.8	46.8	76.3:	35.0:	4.9::	3.8::	109	95.6	187	134
P8 λ 9546	-0.70	1.1:	1.1:	3.0	2.6	6.9	3.5	9.1	4.7	9.5:	4.4:	4.3::	3.3::	5.0:	4.4:	7.9:	5.7:
c			0.00		0.08		0.42		0.40		0.48		0.17		0.08		0.21
$\log F_{H\beta}$ ^b			-12.38		-12.50		-10.76		-10.97		-11.23		-12.20		-12.55		-12.10

^aA single colon indicates uncertainty between 25% and 50%; a double colon indicates uncertainty greater than 50%.

^bergs cm⁻² s⁻¹ in our extracted spectra

Table 2C. Line Strengths^a

Line	f(λ)	F(λ)	I(λ)												
NGC 1535 NGC 2022 NGC 2242 ^b NGC 2371 NGC 2438 NGC 2440 NGC 7027															
[O II] λ 3727	0.29	7.1	7.1	6.8	7.8	48.3	48.3	256	278	115	142	13.4	28.6
He II + H10 λ 3797	0.27	4.3	4.3	3.0	3.4	2.6::	2.6::	2.6::	3.1::	1.9	3.8
He II + H9 λ 3835	0.26	9.0	9.0	8.1	9.2	7.4::	7.4::	10.3	11.1	7.4::	9.0::	3.5	6.9
[Ne III] λ 3869	0.25	101	101	45.4	51.7	10.4	11.9	71.8	71.8	102	110	90.8	110	60.5	116
He I + H8 λ 3889	0.25	21.9	21.9	10.0	11.2	7.4	8.4	13.8	13.8	19.5	20.9	12.7	15.3	8.1	15.5
He ϵ + [Ne III] λ 3968	0.22	75.6	75.6	44.6	49.6	17.6	19.8	61.7	61.7	71.3	76.0	65.3	77.3	28.3	50.7
He I + He II λ 4026	0.21	1.6	1.6	0.9:	1.0:	0.9	0.9	1.2:	1.2:	0.9::	1.1::	1.2	2.0
[S II] λ 4072	0.20	0.6	0.6	1.5	1.6	2.5::	2.5::	2.7::	2.9::	2.9::	3.3::	5.6	9.2
He II + H δ λ 4101	0.19	24.6	24.6	20.9	22.9	19.9	22.0	20.2:	20.2:	20.7	21.8	20.0	22.9	15.4	25.1
He II λ 4198	0.16	1.4	1.5	1.1::	1.3::	0.6	0.8
C II λ 4267	0.14	0.3	0.3	0.8	0.9	0.3	0.4
H γ λ 4340	0.12	46.9	46.9	42.3	44.9	45.7	48.8	45.4	45.4	41.8	43.3	38.7	42.4	32.6	45.0
[O III] λ 4363	0.12	10.6	10.6	10.5	11.1	7.7	8.2	9.9	9.9	7.3	7.5	17.1	18.7	18.2	24.7
He I λ 4471	0.09	3.7	3.7	0.5:	0.5:	0.7::	0.7::	3.0:	3.0:	2.2::	2.4::	2.5	3.2
He II λ 4540	0.07	0.2	0.2	2.9	3.0	3.5	3.6	2.6::	2.6::	1.6:	1.7:	1.3	1.5
N III λ 4640	0.05	2.0	2.0	3.5	3.6	1.3	1.4	5.4	5.6	4.1	4.6
He II λ 4686	0.04	10.6	10.6	87.3	88.8	98.1	100	83.6	83.6	22.1	22.3	50.0	50.8	42.7	46.9
He I + [Ar IV] λ 4711	0.03	3.8	3.8	11.9:	12.1	8.9	9.1:	13.5	13.5	1.1	1.1	8.2	8.4	3.5	3.8
[Ne IV] λ 4724	0.03	1.0:	1.1:	1.1:	1.2:	1.5	1.6
[Ar IV] λ 4740	0.02	2.8	2.8	8.9	9.0	4.6	4.7	10.5	10.5	6.1	6.3	7.8	8.2
H β λ 4861	0.00	100	100	100	100	100	100	100	100	100	100	100	100	100	100
He I λ 4921	-0.02	0.9	0.9	0.1	0.1	0.8::	0.8::	0.6:	0.6:	0.6::	0.6::
[O III] λ 4959	-0.03	320	320	195	192	66.4	65.3	238	238	282	280	411	401	513	474
[O III] λ 5007	-0.04	972	972	653	640	203	199	781	781	959	948	1350	1306	1591	1428
[N I] λ 5199	-0.09	0.4::	0.4::	2.4::	2.3::	13.2	12.3	0.8	0.6
He II λ 5411	-0.13	0.8	0.8	7.9	7.4	8.4	7.8	6.9	6.9	1.7::	1.6::	4.5	4.0	5.7	4.1
[Cl III] λ 5517	-0.16	0.2	0.2	0.4	0.4	0.8::	0.8::	0.7	0.7	0.7::	0.6::	0.3	0.2
[Cl III] λ 5537	-0.16	1.8:	1.7:	1.0	0.6
[O I] λ 5577	-0.17
[N II] λ 5755	-0.21	0.1	0.1	0.8:	0.8:	4.9:	4.6:	17.2	14.7	9.7	5.7

Table 2C—Continued

	NGC 1535 NGC 2022 NGC 2242 ^b NGC 2371 NGC 2438 NGC 2440 NGC 7027																	
Line	f(λ)	F(λ)	I(λ)	F(λ)	I(λ)	F(λ)	I(λ)	F(λ)	I(λ)	F(λ)	I(λ)	F(λ)	I(λ)	F(λ)	I(λ)	F(λ)	I(λ)	
C IV λ 5806	-0.22	0.1::	0.1::	0.2	0.2	0.9	0.5	
He I λ 5876	-0.23	9.6:	9.6:	1.8	1.6	3.5	3.5	10.3:	9.6:	10.0	8.4	20.8	11.4			
He II λ 6005	-0.26	0.1:	0.1:	0.1:	0.1:		
He II λ 6038	-0.26	0.1:	0.1:		
He II λ 6074	-0.27	0.2::	0.1::	0.2	0.1		
[Ca V] λ 6087	-0.27	1.0	0.9	0.2	0.2	0.9	0.5		
[K IV] λ 6101	-0.28	0.1::	0.1::	0.6	0.5	0.6	0.5	0.4:	0.4:	0.2::	0.2::	0.8	0.4			
He II λ 6119	-0.28	0.3	0.2	0.1	...			
He II λ 6172	-0.29	0.3	0.3	0.2::	0.1::	0.3	0.1		
He II λ 6235	-0.30	0.3	0.3	0.2::	0.2::	0.3	0.2		
[O I] λ 6300	-0.31	3.9	3.9	15.8	14.4	25.4	20.0	29.3	13.0			
[S III] λ 6312	-0.32	0.4::	0.4::	2.0	1.7	1.8	1.5	4.3	4.3	1.9::	1.7::	2.5:	3.1:	9.6	4.2			
[O I] λ 6363	-0.32	1.1	1.1	4.6	4.2	7.1	5.6	10.2	4.4			
He II λ 6407	-0.33	0.4	0.4	0.3::	0.3::	0.4	0.2		
[Ar IV] λ 6436	-0.34	1.4	1.2	3.7	3.1	2.7	2.7	1.1:	0.8:	3.8	1.6			
[N II] λ 6548	-0.36	18.2	18.2	70.0	63.2	308	233	71.4	28.2			
H α λ 6563	-0.36	269	269	339	286	346	286	286	286	317	286	378	286	728	286			
[N II] λ 6584	-0.36	0.9	0.9	2.2	1.9	57.3	57.3	239	215	930	703	219	85.2			
He I λ 6678	-0.38	2.5	2.5	1.1	0.9	1.3	1.1	1.8	1.8	2.8	2.5	4.0	3.1	7.5	2.8			
[S II] λ 6716	-0.39	0.1	0.1	0.8	0.7	8.5	8.5	26.4	23.7	11.8	8.7	4.3	1.6			
[S II] λ 6731	-0.39	0.1	0.1	0.9	0.7	9.8	9.8	21.0	18.7	15.9	11.9	9.8	3.6			
He II λ 6891	-0.42	0.7	0.6	1.0	0.8	0.9	0.9	0.6:	0.4:	1.1	0.4			
[Ar V] λ 7005	-0.43	3.2	2.6	8.0	6.3	6.2	6.2	4.5	3.2	9.8	3.2			
He I λ 7065	-0.44	4.4	4.4	0.4	0.3	0.7	0.7	1.9:	1.6:	4.6	3.3	19.4	6.2			
[Ar III] λ 7135	-0.45	6.0	6.0	8.6	7.0	4.0	3.2	18.3	18.3	18.6	16.3	34.4	24.5	65.5	20.2			
He II λ 7178	-0.46	1.0	0.8	1.5:	1.0:	1.4:	0.4:			
[Ar IV] λ 7236	-0.47	0.1	0.1	0.4	0.3	0.6::	0.6::	0.6	0.4	1.9	0.6			
[Ar IV] λ 7264	-0.47	0.4	0.4	0.4	0.4	0.4	0.3	1.1	0.3			
He I λ 7281	-0.47	0.4	0.4	0.1::	0.1::	0.7	0.5	1.9	0.5			
[O II] λ 7323	-0.48	0.5	0.5	0.7	0.6	2.8	2.8	8.3	7.2	19.7	13.7	93.6	26.9			

Table 2C—Continued

		NGC 1535	NGC 2022	NGC 2242 ^b	NGC 2371	NGC 2438	NGC 2440	NGC 7027							
Line		f(λ)	F(λ)	I(λ)	F(λ)	I(λ)	F(λ)	I(λ)	F(λ)	I(λ)	F(λ)	I(λ)	F(λ)	I(λ)	
[Cl IV] λ 7529	-0.51	0.2	0.2	0.7	0.5	1.4	1.1	1.3	1.3	0.5	0.4	1.7	0.5
He II λ 7591	-0.52	1.1	0.8	1.7:	1.3:	1.2	1.2	0.6::	0.4::	2.2	0.6
[S I] λ 7726	-0.54	0.3	0.2	1.0:	0.8:	0.2::	0.2::	0.8	0.2
[Ar III] λ 7751	-0.54	1.1	1.1	2.0	1.6	1.2	0.9	4.6	4.6	5.3	4.6	8.8	5.9	18.3	4.5
[Cl IV] λ 8045	-0.57	0.6	0.6	1.8:	1.3:	1.7	1.3	2.1	2.1	1.2	0.8	4.6	1.0
He II λ 8236	-0.59	1.1	1.1	2.5:	1.9:	4.9	3.6	3.0	3.0	2.4	1.5	4.8	1.0
P17 λ 8467	-0.62	0.3::	0.3::	0.2:	0.1:	1.3:	1.1:	0.7::	0.4::	1.6	0.3
P16 λ 8502	-0.62	0.4::	0.4::	0.5	0.4	0.7:	0.7:	0.9:	0.7:	0.8:	0.5:	2.3	0.5
P15 λ 8544	-0.63	0.4::	0.4::	0.5:	0.3:	1.0:	0.6:	2.6	0.5
P14 λ 8598	-0.63	0.5::	0.5::	0.6:	0.4:	0.4:	0.4:	1.0:	0.6:	3.0	0.6
P13 λ 8664	-0.64	0.6::	0.6::	1.1:	0.8:	2.6	1.9	0.6:	0.6:	1.9:	1.5:	1.7:	1.1:	4.2	0.8
P12 λ 8750	-0.64	0.8::	0.8::	1.1:	0.8:	1.0:	1.0:	1.7:	1.0:	5.3	1.0
P11 λ 8862	-0.65	1.1::	1.1::	1.4:	1.0:	2.3::	1.6::	1.0:	1.0:	2.3:	1.4:	6.8	1.2
P10 λ 9014	-0.67	1.5:	1.5:	1.9:	1.4:	3.8::	2.7::	1.7:	1.7:	2.2:	1.3:	9.8	1.7
[S III] λ 9069	-0.67	1.7:	1.7:	11.6:	8.5:	4.7	3.3	28.3:	28.3:	33.1:	27.3:	27.5	16.6	143.0	25.2
P9 λ 9228	-0.68	2.1:	2.1:	3.4:	2.5:	6.0:	4.2:	3.4:	3.4:	5.3:	3.2:	17.4	3.0
[S III] λ 9532	-0.70	6.8:	6.8:	37.4:	26.9:	10.3:	7.1:	116	116	99.6:	81.6:	85.4	50.5	573	93.4
P8 λ 9546	-0.70	2.2:	2.2:	3.9:	2.8:	5.1:	3.5:	5.2:	5.2:	7.1:	5.8:	8.6:	5.1:	34.4	5.6
c			0.00		0.21		0.23		0.00		0.12		0.34		1.13
log F _{Hβ} ^c		-11.25		-11.62		-12.56		-11.75		-11.85		-10.96		-10.31	

^aA single colon indicates uncertainty between 25% and 50%; a double colon indicates uncertainty greater than 50%.

^bFlux calibration from another night had to be used for wavelengths below 5700Å; night-to-night agreement among calibrations is generally good, and should not affect the line intensities substantially. Intensities relative to H α for lines beyond 5700Å are unaffected.

^cergs cm $^{-2}$ s $^{-1}$ in our extracted spectra

Table 3A. Extinction Quantity c

Object	c(H α)	c(P10)	c(P8)
Hb 12	1.05	1.09	1.02
NGC 3918	0.27	0.18	0.00
NGC 5882	0.41	0.33	0.00
NGC 6567	0.70	0.50	0.65
NGC 6578	1.39	1.12	0.58
NGC 7662	0.03	0.20	0.00
BB1	0.00	0.00	0.00
H4-1	0.08	0.11	0.00
Hu2-1	0.42	0.42	0.39
IC2165	0.40	0.16	0.56
J900	0.48	0.39	0.59
K648	0.17	0.00	0.10
NGC 650A	0.08	0.05	0.19
NGC 650B	0.21	0.24	0.48
NGC 1535	0.00	0.00	0.00
NGC 2022	0.21	0.03	0.03
NGC 2242	0.23	0.46	0.20
NGC 2371	0.00	0.00	0.22
NGC 2438	0.12	0.00	0.41
NGC 2440	0.34	0.11	0.53
NGC 7027	1.13	1.08	1.39

Table 3B. Line Ratios^a

Object	[Ne III]	[O III]	[N II]	[Ar III]	P10/H β	P8/H β	[S III]
Hb 12	2.86	3.13	2.66	4.29	0.020	0.035	2.05
NGC 3918	3.08	3.00	2.38	4.66	0.016	0.014	2.99
NGC 5882	3.15	3.04	2.36	4.54	0.016	0.018	3.49
NGC 6567	7.63	3.06	2.47	4.63	0.014	0.034	3.00
NGC 6578	3.02	3.04	2.92	4.72	0.012	0.010	2.62
NGC 7662	3.27	3.00	2.07	4.16	0.024	0.024	1.92
BB1	1.95	3.38	2.83	...	0.017	0.011	0.80
H4-1	2.91	3.04	3.41	...	0.020	0.026	2.80
Hu2-1	3.02	3.07	3.01	4.31	0.019	0.035	4.16
IC 2165	1.71	3.31	2.71	4.28	0.013	0.047	2.50
J900	1.79	3.29	3.15	4.15	0.016	0.044	2.95
K648	...	3.00	...	2.10	0.014	0.033	...
NGC 650A	1.79	3.31	3.16	4.11	0.018	0.044	2.43
NGC 650B	1.82	3.26	3.06	4.43	0.019	0.057	3.50
NGC 1535	1.69	3.04	...	5.65	0.015	0.022	3.93
NGC 2022	1.54	3.33	...	4.48	0.014	0.028	3.17
NGC 2242	3.11	3.04	...	3.45	0.027	0.035	2.18
NGC 2371	1.57	3.28	3.15	4.02	0.017	0.052	4.10
NGC 2438	1.83	3.39	3.41	3.56	...	0.058	2.98
NGC 2440	1.79	3.26	3.00	4.18	0.013	0.051	3.04
NGC 7027	3.36	3.01	3.02	4.47	0.017	0.056	3.71
Mean	2.64±1.32	3.16±.14	2.87±.38 ^b	4.22±.67	0.017±.006	0.035±.015	2.92±.80
Theory	3.32	2.89	2.95	4.14	0.018	0.037	2.48

^a[Ne III]: $\lambda 3869/\lambda 3968$; [O III]: $\lambda 5007/\lambda 4959$; [N II]: $\lambda 6584/\lambda 6548$; [Ar III]: $\lambda 7135/\lambda 7751$; P10/H β : $\lambda 9014/\lambda 4861$; P8/H β : $\lambda 9546/\lambda 4861$; [S III]: $\lambda 9532/\lambda 9069$. [Ne III] $\lambda 3968$ has been corrected for the expected contribution from He.

^bThe [N II] ratio for NGC 7662 was not used in calculating the mean because the lines are so weak.

Table 4A. Ionic Abundances, Temperatures, & Densities^a

Parameter	Hb 12	NGC 3918	NGC 5882	NGC 6567	NGC 6578	NGC 7662
He ⁺ /H ⁺	7.91E-02	7.03E-02	0.12	0.10	0.12	4.98E-02
He ⁺² /H ⁺	...	4.34E-02	3.31E-03	1.37E-03	1.33E-03	5.53E-02
ICF(He)	1.00	1.00	1.00	1.00	1.00	1.00
O ^o /H ⁺	1.26E-06	7.81E-06	8.26E-07	1.50E-06	6.97E-07	...
O ⁺ /H ⁺	5.30E-06	3.30E-05	8.97E-06	6.81E-06	1.25E-05	2.67E-06
O ⁺² /H ⁺	3.14E-05	3.09E-04	5.24E-04	2.57E-04	7.21E-04	1.94E-04
ICF(O)	1.00	1.62	1.03	1.01	1.01	2.13
N ⁺ /H ⁺	2.87E-06	1.30E-05	2.95E-06	1.81E-06	3.92E-06	4.71E-07
ICF(N)	6.92	16.77	56.93	39.22	59.34	157.34
Ne ⁺² /H ⁺	8.43E-06	6.00E-05	1.41E-04	4.74E-05	2.17E-04	3.30E-05
ICF(Ne)	1.17	1.79	1.05	1.04	1.03	2.16
S ⁺ /H ⁺	2.42E-08	2.34E-07	1.02E-07	5.15E-08	1.06E-07	2.57E-08
S ⁺² /H _{NIR} ⁺	1.59E-06	1.58E-06	3.15E-06	7.66E-07	3.46E-06	1.09E-06
S ⁺² /H ₆₃₁₂ ⁺	6.05E-06	4.14E-06	3.36E-06	8.07E-07	2.68E-06	2.33E-06
S ⁺³ /H _{IR} ⁺ ^d	4.91E-08	3.59E-06	5.90E-06	3.11E-06	7.95E-06	3.64E-06
ICF(S)	1.25	1.46	2.23	1.86	2.20	3.87
Cl ⁺² /H ⁺	3.67E-09	6.64E-08	9.30E-08	2.94E-08	1.41E-07	3.35E-08
Cl ⁺³ /H ⁺	2.86E-09	5.58E-08	7.34E-08	1.84E-08	3.94E-08	6.56E-08
ICF(Cl)	1.00	1.62	1.03	1.01	1.01	2.13
Ar ⁺² /H ⁺	5.52E-07	1.19E-06	1.87E-06	4.11E-07	2.63E-06	4.81E-07
Ar ⁺² /H _{IR} ⁺ ^d	2.60E-07	1.31E-06	1.77E-06	8.65E-07	3.19E-06	5.73E-07
Ar ⁺³ /H ⁺	6.51E-09	7.62E-07	7.96E-07	1.39E-07	4.67E-07	6.66E-07
ICF(Ar)	1.17	1.72	1.05	1.04	1.03	2.14
T _{O3} (K)	18500	12200	9100	11000	7800	12700
T _{N2} (K)	10300	10400	9900	14000	10000	10300
T _{O2} (K)	...	8500	9900	11800	9000	12200
T _{S2} (K)	...	8600	(109600)	16300
T _{S3} (K)	(27300)	15300	10100	14500	9300	13600
N _{e,S2} (cm ⁻³)	6300	3800	2200	6700	2400	2700

^aUnless otherwise noted, uncertainties in ion abundances, electron temperatures, and electron densities are ±30%, ±10%, and ±10%, respectively.

^b±50%

^c±75%

^dS⁺³ and Ar⁺² abundances were computed using the measured strengths of 10.5 μ and 8.99 μ , respectively (see text).

Table 4B. Ionic Abundances, Temperatures, & Densities^a

Parameter	BB1	H4-1	Hu2-1	IC2165	J900	K648	NGC 650A	NGC 650B
He ⁺ /H ⁺	7.12E-02	0.11	0.10	5.53E-02	6.26E-02	9.52E-02	5.55E-02	8.31E-02
He ⁺² /H ⁺	1.88E-02	8.70E-03	1.66E-04	3.65E-02	3.25E-02	...	5.06E-02	2.62E-02
ICF(He)	1.00	1.00	1.00	1.00	1.00	1.00	1.00	1.00
O ^o /H ⁺	7.95E-07	1.69E-05	2.29E-06	2.56E-06	7.21E-06	...	2.77E-05	6.91E-05
O ⁺ /H ⁺	5.08E-06	5.99E-05	3.00E-05	9.52E-06	1.88E-05	1.90E-05	1.00E-04	2.14E-04
O ⁺² /H ⁺	5.64E-05	1.26E-04	2.13E-04	1.78E-04	2.14E-04	5.15E-05	3.23E-04	2.51E-04
ICF(O)	1.26	1.08	1.00	1.66	1.52	1.00	1.91	1.31
N ⁺ /H ⁺	3.88E-06	1.75E-05	9.71E-06	4.07E-06	5.40E-06	7.65E-07	5.72E-05	1.11E-04
ICF(N)	15.30	3.33	8.12	32.71	18.85	3.71	8.06	2.86
Ne ⁺² /H ⁺	9.17E-05	2.45E-06	2.67E-05	3.93E-05	5.34E-05	7.00E-06	1.02E-04	1.14E-04
ICF(Ne)	1.38	1.59	1.14	1.75	1.65	1.37	2.51	2.43
S ⁺ /H ⁺	7.78E-09	3.96E-08	5.53E-08	1.00E-07	1.68E-07	7.66E-09	1.48E-06	2.56E-06
S ⁺² /H _{NIR} ⁺	4.68E-08	1.16E-07	1.12E-06	1.47E-06	1.31E-06	1.99E-07	3.95E-06	6.57E-06
S ⁺² /H ₆₃₁₂ ⁺	...	3.98E-07	6.38E-07	1.87E-06	1.77E-06	...	1.00E-05	8.55E-06
ICF(S)	1.43	1.14	1.27	1.75	1.50	1.15	1.27	1.12
Cl ⁺² /H ⁺	4.11E-08
Cl ⁺³ /H ⁺	4.04E-08	2.45E-08	...	4.05E-08	8.69E-09
ICF(Cl)	1.26	1.08	1.00	1.66	1.52	1.00	1.91	1.31
Ar ⁺² /H ⁺	9.70E-09	2.41E-08	1.18E-06	5.26E-07	4.93E-07	4.13E-08	2.14E-06	2.30E-06
Ar ⁺³ /H ⁺	4.05E-07	2.55E-07	...	3.49E-07	5.28E-08
ICF(Ar)	1.35	...	1.14	1.71	1.60	...	2.18	...
T _{O3} (K)	12400	12300	9100	13000	11600	11800	10800	11100
T _{N2} (K)	11700	10200	13500	12700	11500	9200	9700	9600
T _{O2} (K)	8000	6100	20600	9800	10300	8400	14800	14500
T _{S2} (K)	...	(42700)	(33000)	10300	7800	...	10300	10200
T _{S3} (K)	...	(23000)	11100	14200	13000	...	13300	10400
N _{e,S2} (cm ⁻³)	7100	400	8500	4100	3600	1000 ^d	200	200

^aUnless otherwise noted, uncertainties in ion abundances, electron temperatures, and electron densities are ±30%, ±10%, and ±10%, respectively.

^b±50%

^c±75%

^d[S II] density reported by Henry, Kwitter, & Bates (2000) was used, since lines at 6716Å and 6731Å were not measured here.

Table 4C. Ionic Abundances, Temperatures, & Densities^a

Parameter	NGC 1535	NGC 2022	NGC 2242	NGC 2371	NGC 2438	NGC 2440	NGC 7027
He ⁺ /H ⁺	7.38E-02	1.15E-02	...	2.55E-02	7.40E-02	5.76E-02	6.09E-02
He ⁺² /H ⁺	9.79E-03	8.07E-02	0.10	7.72E-02	2.04E-02	4.73E-02	4.26E-02
ICF(He)	1.00	1.00	1.00	1.00	1.00	1.00	1.00
O ^o /H ⁺	1.06E-05	2.52E-05	2.93E-05	4.50E-06
O ⁺ /H ⁺	3.07E-07	2.29E-06	...	3.33E-05	9.34E-05	5.35E-05	1.89E-05
O ⁺² /H ⁺	2.34E-04	9.15E-05	1.16E-05	1.58E-04	3.18E-04	2.32E-04	2.25E-04
ICF(O)	1.13	8.00	1.00	4.02	1.28	1.82	1.70
N ⁺ /H ⁺	6.17E-08	2.65E-07	...	1.31E-05	3.98E-05	1.10E-04	1.06E-05
ICF(N)	867.45	327.35	1.00	23.17	5.62	9.71	21.92
Ne ⁺² /H ⁺	6.30E-05	1.72E-05	1.32E-06	3.66E-05	1.02E-04	4.78E-05	3.85E-05
ICF(Ne)	1.13	8.20	1.00	4.87	1.65	2.24	1.84
S ⁺ /H ⁺	9.83E-10	2.74E-08	...	5.76E-07	9.27E-07	4.92E-07	6.37E-07
S ⁺² /H _{NIR} ⁺	2.93E-07 ^d	1.06E-06	2.29E-07	4.15E-06	4.50E-06	1.64E-06	2.92E-06
S ⁺² /H ₆₃₁₂ ⁺	1.16E-07	2.99E-06	1.90E-06	1.67E-05	3.95E-06	3.69E-06	1.43E-06
ICF(S)	22.22	7.16	...	1.58	1.21	1.31	1.55
Cl ⁺² /H ⁺	1.13E-07	5.77E-08
Cl ⁺³ /H ⁺	3.76E-08	5.70E-08	2.81E-08	1.17E-07	...	3.81E-08	4.23E-08
ICF(Cl)	1.13	8.00	1.00	4.02	1.28	1.82	1.70
Ar ⁺² /H ⁺	4.14E-07	3.26E-07	7.73E-08	1.12E-06	1.43E-06	1.34E-06	9.43E-07
Ar ⁺³ /H ⁺	4.19E-07	8.29E-07	1.94E-07	1.30E-06	...	6.64E-07	5.75E-07
ICF(Ar)	1.13	8.02	...	4.21	1.55	2.03	1.78
T _{O3} (K)	11400	13600	21300	12100	10300	12600	13600
T _{N2} (K)	(30500)	10300	10300	8600	10400	10300	20100
T _{O2} (K)	7400	7500	...	6800	13100	8300	...
T _{S2} (K)	11400	9700	13800	...
T _{S3} (K)	17900	19600	(284000)	13300	10000	13800	15100
N _{e,S2} (cm ⁻³)	300	800	1300 ^e	1000	200	1800	81000

^aUnless otherwise noted, uncertainties in ion abundances, electron temperatures, and electron densities are ±30%, ±10%, and ±10%, respectively.

^b±50%

^c±75%

^d[O III] temperature used to calculate this abundance.

^e[S II] electron density from Howard, Henry, & McCartney (1997) was used, since line at 6716Å was not measured here.

Table 5. S^{+3} Abundance Comparisons

Object	$S^{+3}/H^+(ICF)$	$S^{+3}/H^+(IR)$	ICF/IR
Hb 12	4.03E-7: ^a	4.91E-8:: ^b	8.22::
NGC 3918	8.34E-7	3.59E-6::	0.23::
NGC 5882	4.00E-6	5.90E-6	0.68
NGC 6567	7.03E-7	3.11E-6	0.22
NGC 6578	4.28E-6	7.95E-6:	0.54:
NGC 7662	3.20E-6	3.64E-6	0.88

^aA single colon represents an estimated uncertainty between 25% and 50%.

^bA double colon represents an estimated uncertainty greater than 50%.

Table 6A. Elemental Abundances

Element	Hb 12	NGC 3918	NGC 5882	NGC 6567	NGC 6578	NGC 7662	Sun ^a	Orion ^b
He/H	0.08(±.01)	0.11(±.01)	0.12(±.01)	0.10(±.01)	0.12(±.01)	0.10(±.01)	0.10	0.10
O/H ($\times 10^4$)	0.37(±.05)	5.54(±.78)	5.48(±.77)	2.67(±.38)	7.42(±1.0)	4.19(±.59)	7.41	5.25
N/H ($\times 10^4$)	0.20(±.04)	2.18(±.45)	1.80(±.37)	0.71(±.15)	2.33(±.43)	0.74(±.16)	0.93	0.60
Ne/H ($\times 10^4$)	0.10(±.02)	1.07(±.23)	1.48(±.30)	0.49(±.11)	2.23(±.42)	0.71(±.13)	1.20	0.78
S/H ($\times 10^5$) ^c	0.20(±.07)	0.26(±.06)	0.72(±.15)	0.15(±.03)	0.79(±.18)	0.43(±.07)	2.14	1.48
S/H ($\times 10^5$) ^d	0.17(±.06)	0.54(±.13)	0.91(±.19)	0.39(±.09)	1.15(±.26)	0.48(±.08)	2.14	1.48
Cl/H ($\times 10^7$)	0.07(±.04)	1.98(±.39)	1.71(±.33)	0.48(±.17)	1.82(±.63)	2.11(±.42)	3.16	2.14
Ar/H ($\times 10^6$)	0.65(±.41)	3.36(±.69)	2.79(±.55)	0.57(±.11)	3.18(±.62)	2.46(±.48)	3.31	3.09
N/O	0.54(±.08)	0.39(±.06)	0.33(±.05)	0.27(±.04)	0.31(±.04)	0.18(±.03)	0.13	0.11
Ne/O	0.27(±.04)	0.19(±.03)	0.27(±.04)	0.18(±.03)	0.30(±.04)	0.17(±.02)	0.16	0.15
S/O ($\times 10^1$) ^d	0.55(±.17)	0.05(±.01)	0.13(±.02)	0.06(±.01)	0.11(±.02)	0.10(±.01)	0.29	0.28
Cl/O ($\times 10^3$)	0.18(±.11)	0.36(±.05)	0.31(±.04)	0.18(±.06)	0.25(±.08)	0.50(±.07)	0.43	0.41
Ar/O ($\times 10^2$)	1.78(±1.1)	0.61(±.09)	0.51(±.07)	0.21(±.03)	0.43(±.06)	0.59(±.08)	0.45	0.59

^aGrevesse et al. (1996)

^bEsteban et al. (1998), Table 19, gas + dust

^cSulfur abundance based upon ICF method

^dSulfur abundance based upon S⁺³ ion abundance

Table 6B. Elemental Abundances

Element	BB1	H4-1	Hu2-1	IC2165	J900	K648	NGC 650A	NGC 650B	Sun ^a	Orion ^b
He/H	0.09(±.01)	0.12(±.02)	0.10(±.01)	0.09(±.01)	0.10(±.01)	0.10(±.01)	0.11(±.02)	0.11(±.02)	0.10	0.10
O/H ($\times 10^4$)	0.78(±.11)	1.99(±.28)	2.43(±.34)	3.11(±.44)	3.54(±.50)	0.71(±.10)	8.10(±1.1)	6.11(±.86)	7.41	5.25
N/H ($\times 10^4$)	0.59(±.27)	0.58(±.11)	0.79(±.17)	1.33(±.26)	1.02(±.20)	0.03(±.01)	4.61(±.65)	3.16(±.65)	0.93	0.60
Ne/H ($\times 10^4$)	1.26(±.25)	0.04(±.02)	0.31(±.06)	0.69(±.14)	0.88(±.19)	0.10(±.02)	2.57(±.53)	2.78(±.57)	1.20	0.78
S/H ($\times 10^5$)	0.01(±.01)	0.02(±.003)	0.15(±.03)	0.27(±.05)	0.22(±.08)	0.02(±.01)	0.69(±.12)	1.02(±.23)	2.14	1.48
Cl/H ($\times 10^7$)	0.41(±.13)	0.67(±.13)	0.37(±.09)	...	0.77(±.25)	0.11(±.04)	3.16	2.14
Ar/H ($\times 10^6$)	0.01(±.005)	0.02(±.003)	1.34(±.27)	1.60(±.32)	1.20(±.24)	0.04(±.009)	5.44(±1.04)	2.30(±.43)	3.31	3.09
N/O	0.76(±.11)	0.29(±.04)	0.32(±.05)	0.43(±.06)	0.29(±.04)	0.04(±.01)	0.57(±.02)	0.52(±.08)	0.13	0.11
Ne/O	1.63(±.23)	0.02(±.01)	0.13(±.02)	0.22(±.03)	0.25(±.04)	0.14(±.02)	0.32(±.05)	0.46(±.07)	0.16	0.15
S/O ($\times 10^1$)	0.01(±.01)	0.01(±.001)	0.06(±.01)	0.09(±.01)	0.06(±.02)	0.03(±.02)	0.09(±.01)	0.17(±.03)	0.29	0.28
Cl/O ($\times 10^3$)	0.17(±.05)	0.22(±.03)	0.11(±.02)	...	0.10(±.03)	0.02(±.007)	0.43	0.41
Ar/O ($\times 10^2$)	0.02(±.01)	0.01(±.001)	0.55(±.08)	0.51(±.07)	0.34(±.05)	0.06(±.01)	0.67(±.09)	0.38(±.05)	0.45	0.59

^aGrevesse et al. (1996)

^bEsteban et al. (1998), Table 19, gas + dust

Table 6C. Elemental Abundances

Element	NGC 1535	NGC 2022	NGC 2242	NGC 2371	NGC 2438	NGC 2440	NGC 7027	Sun ^a	Orion ^b
He/H	0.08(±.01)	0.09(±.01)	0.10(±.01)	0.10(±.01)	0.09(±.01)	0.10(±.01)	0.10(±.01)	0.10	0.10
O/H ($\times 10^4$)	2.66(±.38)	7.50(±1.1)	0.12(±.02)	7.71(±1.1)	5.24(±.74)	5.19(±.73)	4.15(±.59)	7.41	5.25
N/H ($\times 10^4$)	0.54(±.11)	0.87(±.19)	...	3.03(±.64)	2.23(±.44)	10.67(±2.13)	2.33(±.47)	0.93	0.60
Ne/H ($\times 10^4$)	0.71(±.15)	1.41(±.30)	0.01(±.005)	1.78(±.34)	1.69(±.36)	1.07(±.21)	0.71(±.13)	1.20	0.78
S/H ($\times 10^5$)	0.65(±.23)	0.78(±.26)	...	0.74(±.25)	0.66(±.22)	0.28(±.07)	0.55(±.16)	2.14	1.48
Cl/H ($\times 10^7$)	0.43(±.08)	4.56(±1.57)	0.28(±.06)	4.72(±.97)	...	2.75(±.96)	1.70(±.35)	3.16	2.14
Ar/H ($\times 10^6$)	0.94(±.19)	9.27(±1.91)	...	10.19(±2.07)	2.22(±.45)	4.06(±.81)	2.70(±.54)	3.31	3.09
N/O	0.20(±.03)	0.12(±.02)	...	0.39(±.06)	0.43(±.06)	2.05(±.29)	0.56(±.08)	0.13	0.11
Ne/O	0.27(±.04)	0.19(±.03)	0.11(±.02)	0.23(±.03)	0.32(±.05)	0.21(±.03)	0.17(±.02)	0.16	0.15
S/O ($\times 10^1$)	0.25(±.08)	0.10(±.03)	...	0.10(±.03)	0.13(±.04)	0.05(±.01)	0.13(±.02)	0.29	0.28
Cl/O ($\times 10^3$)	0.16(±.02)	0.61(±.19)	2.41(±.34)	0.61(±.09)	...	0.53(±.17)	0.41(±.06)	0.43	0.41
Ar/O ($\times 10^2$)	0.36(±.05)	1.24(±.18)	...	1.32(±.19)	0.42(±.06)	0.78(±.11)	0.65(±.09)	0.45	0.59

^aGrevesse et al. (1996)

^bEsteban et al. (1998), Table 19, gas + dust

Table 7. Comparison of Abundance Averages

Ratio	This Paper	Paper I	Paper IIB	KB ^a	AK ^b	Sun ^c	Orion ^d
O/H (x 10 ⁴)	4.1±2.5	5.5±1.5	5.4±1.9	4.8±2.0	4.4±.19	7.41	5.25
S/O (x 10 ¹)	0.11±.11	0.13±0.073	0.11±0.064	0.17±.14	0.25±.022	0.29	0.28
Cl/O (x 10 ³)	0.42±.53	0.33±0.15	0.31±0.12	...	0.47±.04	0.43	0.41
Ar/O (x 10 ²)	0.57±.43	0.51±0.18	0.51±0.20	0.48±.48	0.69±.05	0.45	0.59

^aAverage abundance ratios for a sample of planetary nebulae from Kingsburgh & Barlow (1994)

^bAverage abundance ratios for a sample of planetary nebulae from Aller & Keyes (1987)

^cGrevesse et al. (1996)

^dEsteban et al. (1998), Table 19, gas + dust

REFERENCES

- Aller, L.H., & Keyes, C.D. 1987, ApJS, 65, 405
- Esteban, C., Peimbert, M., Torres-Peimbert, S., & Escalante, V. 1998, MNRAS, 295, 401
- Grevesse, N., Noels, A., & Sauval, A.J. 1996, in ASP Conf. Ser. 99, Cosmic Abundances, ed. S.S. Holt & G. Sonneborn (San Francisco: ASP), 117
- Henry, R.B.C., Kwitter, K.B., & Bates, J.A. 2000, ApJ, 531, 928
- Howard, J.W., Henry, R.B.C., & McCartney, S. 1997, MNRAS, 284, 465
- Hummer, D.G., & Storey, P.J. 1987, MNRAS, 224, 801
- Hyung, S., & Aller, L.H. 1996, MNRAS, 278, 551
- Kingsburgh, R.L., & Barlow, M.J. 1994, MNRAS, 271, 257
- Kwitter, K.B., & Henry, R.B.C. 1998, ApJ, 493, 247
- Kwitter, K.B., & Henry, R.B.C. 2001, ApJ, 562, 804 (Paper I)
- Mendoza, C. 1983, in IAU Symp. 103, Planetary Nebulae, ed. D.R. Flower (Dordrecht: Reidel), 143
- Milingo, J.B., Kwitter, K.B., Henry, R.B.C., & Cohen, R.E. 2002, ApJS, 138, 279 (Paper IIA)
- Milingo, J.B., Henry, R.B.C., & Kwitter, K.B. 2002, ApJS, 138, 285 (Paper IIB)
- Osterbrock, D.E. 1989, *Astrophysics of Gaseous Nebulae and Active Galactic Nuclei*, (Mill Valley, CA: University Science Books)
- Rieke, G.H., & Lebofsky, M.J. 1985, ApJ, 288, 618

Savage, B.D., & Mathis, J.S. 1979, ARA&A, 17, 73

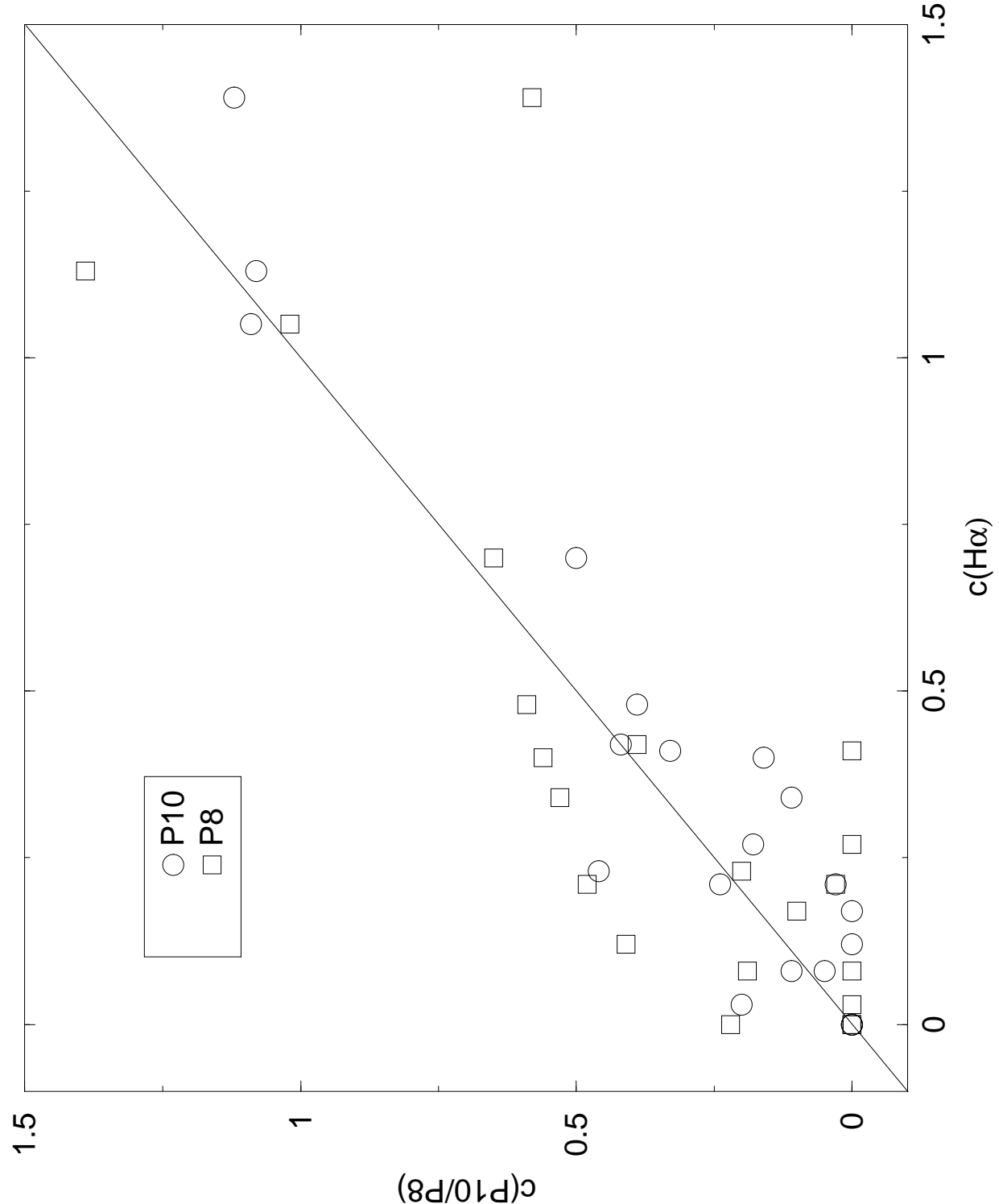
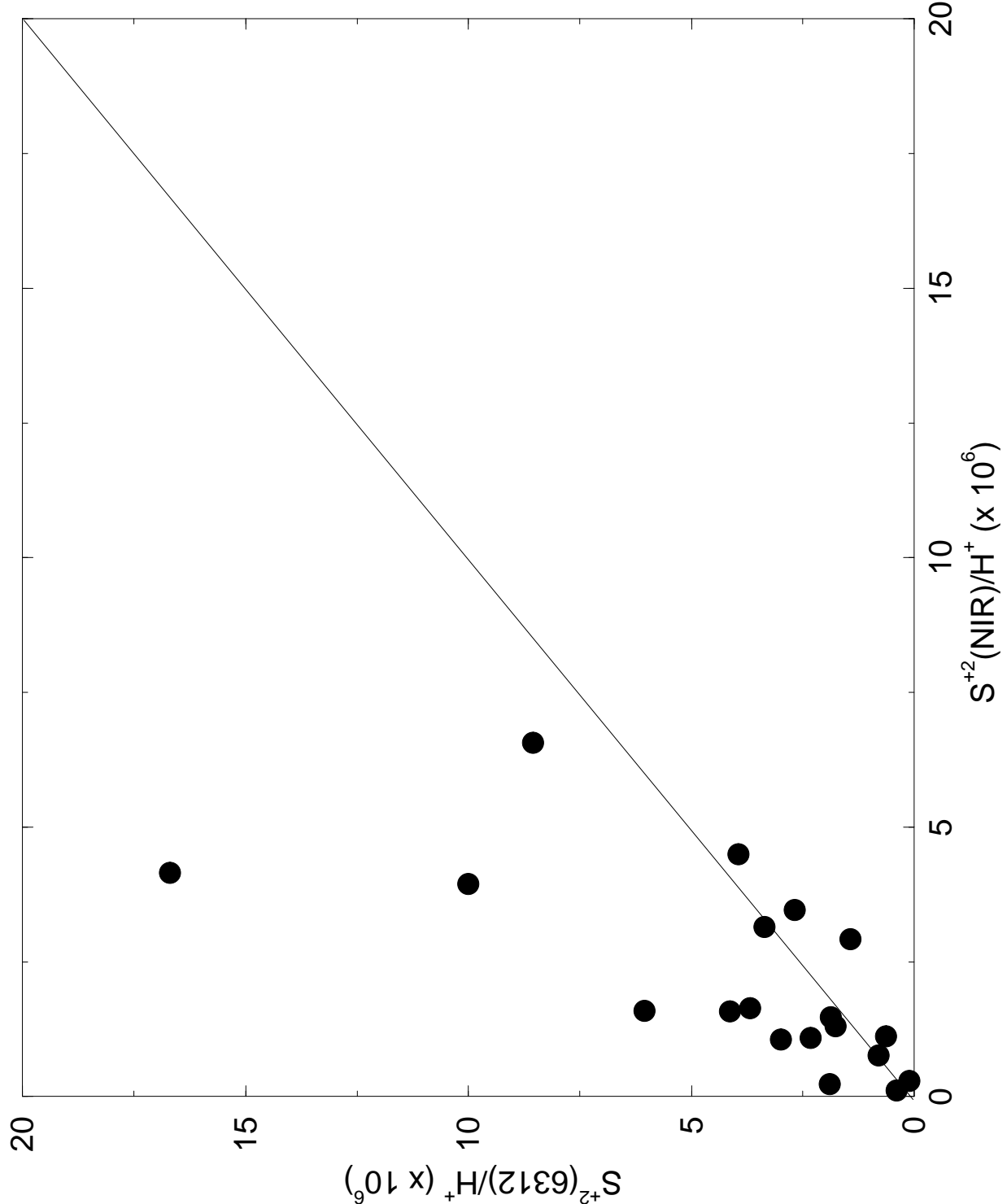


Fig. 1.— A comparison of logarithmic extinction c as determined using the Paschen 8 and 10 lines versus the value inferred from using $H\alpha$. The solid line shows the track for a one-to-one correspondence.



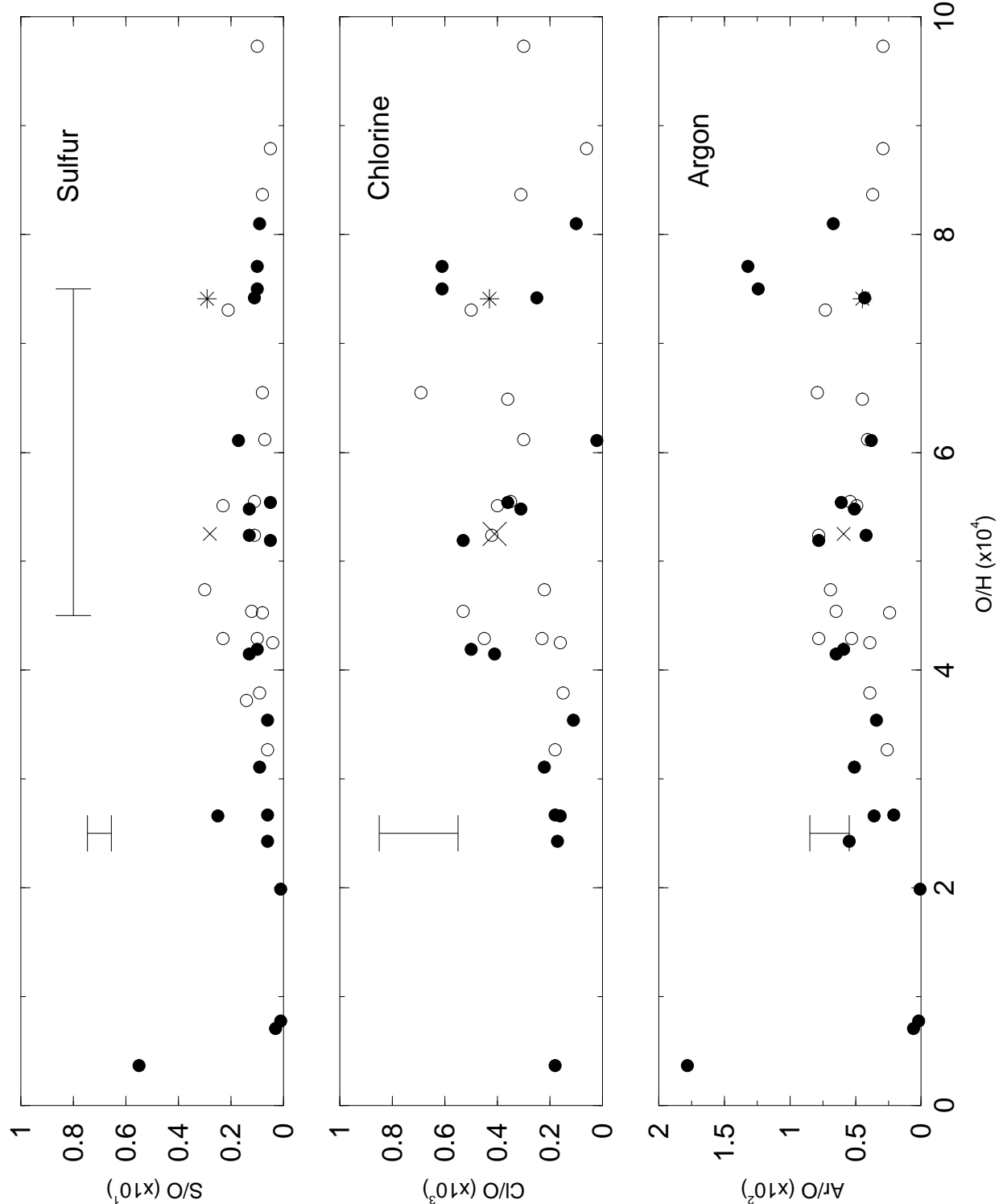


Fig. 3.— Top: $S/O (x 10^1)$ versus $O/H (x 10^4)$, where filled circles are ratios determined in this paper, open circles are ratios from Paper 1. The position of the sun (Grevesse et al. 1996) and the Orion Nebula (Esteban et al. 1998) are indicated with a star and an X, respectively. Middle: Same as top but for $Cl/O (x 10^3)$. Bottom: Same as top but for $Ar/O (x 10^2)$. Ordinate uncertainties are shown with error bars in each panel, while the horizontal